HHS Public Access

Author manuscript

Gut. Author manuscript; available in PMC 2019 April 01.

Published in final edited form as:

Gut. 2019 April ; 68(4): 684–692. doi:10.1136/gutjnl-2017-315920.

Genetic editing of colonic organoids provides a molecularly distinct and orthotopic preclinical model of serrated carcinogenesis

Tamsin RM Lannagan[1], **Young K Lee**[1], **Tongtong Wang**[1], **Jatin Roper**[2,3], **Mark L Bettington**[4,5], **Lochlan Fennell**[5], **Laura Vrbanac**[1], **Lisa Jonavicius**[6], **Roshini Somashekar**[1], **Krystyna Gieniec**[1], **Miao Yang**[1], **Jia Q Ng**[1], **Nobumi Suzuki**[1], **Mari Ichinose**[1], **Josephine A Wright**[1], **Hiroki Kobayashi**[1], **Tracy L Putoczki**[7], **Yoku Hayakawa**[8], **Simon Leedham**[9], **Helen E Abud**[10], **Ömer H. Yilmaz**[2,11], **Julie Marker**[12], **Sonja Klebe**[6], **Pratyaksha Wirapati**[13], **Siddhartha Mukherjee**[14], **Sabine Tejpar**[15], **Barbara A Leggett**[5,16,17], **Vicki LJ Whitehall**[5,16,18], **Daniel L Worthley**[1,*], and **Susan L Woods**[1,*]

[1]School of Medicine, University of Adelaide and South Australian Health and Medical Research Institute, Adelaide, SA Australia [2]The David H. Koch Institute for Integrative Cancer Research at MIT, Cambridge, MA [3]Division of Gastroenterology, Tufts Medical Center, Boston, MA, United States [4]Envoi Specialist Pathologists, Brisbane, QLD Australia [5]QIMR Berghofer Medical Research Institute, Brisbane, QLD Australia [6]Department of Anatomical Pathology, Flinders Medical Centre, Bedford Park, SA Australia [7]Department of Medical Biology, University of Melbourne and the Walter and Eliza Hall Institute of Medical Research, Melbourne, VIC Australia [8]Dept of Gastroenterology, University of Tokyo, Japan [9]Gastrointestinal Stem Cell Biology Laboratory, Wellcome Trust Centre for Human Genetics University of Oxford, Oxford, & Translational Gastroenterology Unit, Experimental Medicine Division, Nuffield Department of Clinical Medicine, John Radcliffe Hospital, Oxford, Headington, UK [10]Cancer Program, Monash Biomedicine Discovery Institute and the Department of Anatomy and Developmental Biology, Monash University, Clayton, VIC Australia [11]Department of Pathology, Massachusetts General Hospital, Boston, MA United States [12]Cancer Voices SA, SA Australia [13]Swiss Institute of Bioinformatics, Bioinformatics Core Facility, Lausanne, Switzerland [14]Department of Medicine, Columbia University Medical Center, New York, NY, USA [15]Digestive Oncology Unit, Department of Oncology, University Hospitals Leuven, Leuven, Belgium [16]School of Medicine, University of Queensland, QLD Australia [17]Royal Brisbane and Womens Hospital, Brisbane, QLD Australia [18]Pathology Queensland, Brisbane, QLD

Abstract

Objective—Serrated colorectal cancer (CRC) accounts for approximately 25% of cases, and includes tumours that are amongst the most treatment resistant and with worst outcomes. This

[*]**Dual corresponding author details:** Dr. Susan Woods, PhD., Postal address- GICB Lab, Level 5 South, South Australian Health & Medical Research Institute (SAHMRI), North Terrace, Adelaide SA 5000, AUSTRALIA, p: (08) 8128 4386 m: 0488 737408 susan.woods@adelaide.edu.au, Dr. Daniel Worthley, MBBS(Hons), PhD, MPH, FRACP., Postal address- GICB Lab, Level 5 South, South Australian Health & Medical Research Institute (SAHMRI), North Terrace, Adelaide SA 5000, AUSTRALIA, p: (08) 8128 4386 m: 0400 363208 Dan.worthley@sahmri.com.

CRC subtype is associated with activating mutations in the mitogen activated kinase (MAPK) pathway gene, *BRAF*, and epigenetic modifications termed the CpG Island Methylator Phenotype (CIMP), leading to epigenetic silencing of key tumour suppressor genes. It is still not clear which (epi-)genetic changes are most important in neoplastic progression and we begin to address this knowledge gap herein.

Design—We utilise organoid culture combined with CRISPR/Cas9 genome engineering, to sequentially introduce genetic alterations associated with serrated CRC and which regulate the stem cell niche, senescence and DNA mismatch repair.

Results—Targeted biallelic gene alterations were verified by DNA sequencing. Organoid growth in the absence of niche factors was assessed, as well as analysis of downstream molecular pathway activity. Orthotopic engraftment of complex organoid lines, but not $Braf^{V600E}$ alone, quickly generated adenocarcinoma *in vivo* with serrated features consistent with human disease. Loss of the essential DNA mismatch repair enzyme, Mlh1, led to microsatellite instability. Sphingolipid metabolism genes are differentially regulated in both our mouse models of serrated CRC and human CRC, with key members of this pathway having prognostic significance in the human setting.

Conclusion—We generate rapid, complex models of serrated CRC to determine the contribution of specific genetic alterations to carcinogenesis. Analysis of our models alongside patient data has led to the identification of a potential susceptibility for this tumour type.

INTRO

Sporadic colorectal cancer (CRC) develops via two main genetic pathways. The conventional pathway described by Fearon & Vogelstein [1] has characteristic chromosomal instability (CIN) with stepwise loss of key tumour suppressors (eg. *Adenomatous polyposis coli*, *APC*) and activation of oncogenes (eg. *KRASG12D* mutation). In the last two decades, an alternate molecular pathway has been identified that accounts for 25% of CRC [2]. This subtype of CRC is named for the serrated, or saw-toothed, morphology of the precursor lesion, including sessile serrated polyps, and comprises a molecularly distinct, somewhat heterogeneous tumour type that forms without CIN. It can be best differentiated from conventional CRC by two characteristic molecular markers; the presence of the $BRAF^{V600E}$ mutation that activates the mitogen-activated protein kinase (MAPK) pathway and the coincident, coordinated epigenetic modification of specific target promoters termed the CpG Island Methylator Phenotype (CIMP) [3]. $BRAF^{V600E}$/$CIMP^{+}$ tumours account for 8–20% of all CRC [2, 4]. These are preferentially located in the proximal colon, frequently present with higher grade and contain a group of cancers with the worst prognosis of all CRC [2, 5]. Furthermore, of relevance to the gastrointestinal cancer preventionist, these serrated lesions are less well detected by current CRC screening programs and are overrepresented in colonoscopic interval cancers [6, 7]. The molecular basis for these subtype characteristics are not well understood, but may hold the key to preventing and treating serrated CRC.

The culture of normal and tumour derived organoids pioneered by Hans Clevers and his group [8, 9] allows the indefinite, *in vitro* propagation of primary gut epithelia and neoplastic specimens. Cells are grown in self-organising aggregates with representative

epithelial architecture, suspended within a basement membrane-gel matrix and supported by stem cell niche signalling factors. For the colon these factors, Wnt/R-spondin, Epidermal growth factor (EGF), and Noggin activate the Wnt and MAPK pathways and inhibit the bone morphogenic protein (BMP) pathway, respectively. This culture system supports the stem cell population, as well as more differentiated cell types, allowing long-term primary culture containing many of the representative epithelial cell types of the original tissue.

The next-generation sequencing revolution has armed us with more information than ever before about the (epi-)genetic changes associated with serrated CRC. Mining this static data is relatively simple, yet understanding the contribution of genetic events to carcinogenesis is a real challenge. To this end, we have combined recent advances in stem cell biology [10] with genome editing techniques [11], to produce a system in which multiple genetic alterations can be assessed for their contribution to serrated CRC. This is analogous to the approach taken to model the conventional pathway to CRC [12, 13] and is inspired by the observation that many recurrent CRC mutations lie within genes involved in key signalling pathways that are essential for maintenance of the intestinal stem cell niche [14]. Our work provides new insights into the importance of common (epi-)genetic alterations found in human serrated CRC and highlights a potential vulnerability of this cancer type.

RESULTS

To identify recurrent serrated CRC associated alterations in stem cell niche signalling and senescence pathways, we analysed The Cancer Genome Atlas (TCGA) (epi-)genomic data for 633 CRC cases [15]. $BRAF^{V600E}$ mutation is estimated to mark 50–67% of serrated CRCs [2] and, in the absence of microsatellite instability (MSI), is associated with poor outcome for late stage disease [2, 16]. As only 30% of serrated CRCs retain serrated crypt morphology [2], we use the $BRAF^{V600E}$ molecular marker rather than histological appearance to extract serrated CRC cases from the TCGA set. In the 50 TCGA CRC cases that contain $BRAF^{V600E}$ (depicted in Figure 1), we then used a candidate gene approach to look for frequently co-altered genes that play important roles in regulating the stem cell niche or senescence. *p16 INK4A* encodes a tumour suppressor protein critical for oncogene induced senescence. Loss of *p16 INK4a* expression is associated with the conversion of serrated polyps to high-grade dysplasia/CRC and cooperates with $Braf^{V600E}$ in a mouse model of serrated CRC [17, 18, 19]. Consistent with previous reports, we detected *p16 INK4A* hypermethylation or mutation in 46% of TCGA CRC cases overall and in 84% of $BRAF^{V600E}$ CRC (Figure 1) [20, 21, 22]. The Wnt pathway intricately regulates intestinal stem cell proliferation and differentiation. The classic Wnt-pathway regulator, *APC*, is the most commonly mutated gene in CRC [15]. However for $BRAF^{V600E}$ CRC, we identified two negative regulators, *ZNRF3* and *RNF43*, as the most commonly altered Wnt pathway genes (Figure 1) [23]. Interestingly, in mice, cooperative inactivation of both *Rnf43* and *Znrf3* are required for polyp formation [24] and we detect alteration of both genes in 32% of $BRAF^{V600E}$ CRC. This is consistent with reports of differential Wnt pathway disruption in precursor lesions of the serrated pathway to CRC compared to the conventional pathway [25, 26]. The mutation rate of *RNF43* is likely under-represented in the TCGA dataset due to incomplete calling of frame-shift mutations because of their similarity to technical DNA polymerase slippage errors [27]. The transforming growth factor-β (TGFβ) pathway is

frequently aberrantly regulated in CRC, often through mutation of *TGFβ receptor 2* (*TGFβR2*) [15]. *TGFβR2* mutation occurred in 10% of the $BRAF^{V600E}$ CRC cases we examined (Figure 1), again reflecting under calling of the polyadenine repeat tract mutations in the TCGA dataset as use of older sequencing modalities identified *TGFBR2* as mutated in 90% of MSI CRC [28]. Lastly, we wanted to model MSI CRC and so examined the key mismatch repair gene, *MutL homolog 1* (*MLH1*). In line with a meta-analysis of *MLH1* methylation frequency in CRC, we detected *MLH1* hypermethylation in 20% of TCGA CRC cases [29]. This increased to 74% alteration in $BRAF^{V600E}$ CRC (Figure 1).

Carcinogenesis is a story of liberation and, as we genetically engineer successive stages of serrated CRC, we select organoids through their unique biology, microenvironmental requirements and treatment sensitivities. Firstly, the $BRAF^{V600E}$ mutation is an early genetic change in serrated polyps [30]. To first incorporate this mutation, we established colon organoid cultures from $BRAF^{CA}/Villin^{CreERT}$ mice (Figure 2). *In vitro* treatment with 4-hydroxytamoxifen (4-OHT) induced highly efficient recombination to $Braf^{V600E}$ (Supplementary Figure 1) and activation of ERK1/2 phosphorylation (Figure 2A). This *in vitro* system mimics the chemoresistance to epidermal growth factor receptor (EGFR) inhibitors observed for MAPK mutant CRC in the clinic [31]. Treatment with EGFR inhibitor results in a significant growth inhibition of wild-type organoids in culture but not $Braf^{V600E}$ organoids (Figure 2B, Supplementary Figure 2).

Genome editing using microbial Cas9 nucleases from the clustered regularly interspaced short palindromic repeats (CRISPR) adaptive immune system has revolutionised the field of genome editing [11]. We have modelled serrated CRC using this genome editing technique. Thus, following mutation of *Braf* we sequentially incorporated 4 further genetic alterations using CRISPR/Cas9 [11] (Figure 2). Similar to previous work [12, 13], the addition of Tgfβ to culture medium selected for organoids with functional loss of the Tgfβ pathway, in this case Tgfβr2 ($Braf^{V600E}$; $Tgfbr2^{\Delta/\Delta}$, abbreviated to $Braf^{V600E}\Delta T$) (Figure 2B). Indeed, wild type (WT), $Braf^{V600E}$ and control transfected cultures do not survive in the presence of Tgfβ [32] (Figure 2B). Quantitative real-time PCR (qRT-PCR) analysis of the Tgfβ response gene, *Serpin1*, showed that Tgfβ can activate this pathway in $Braf^{V600E}$ organoids as shown by an increase in *Serpin1* mRNA levels. However, organoids containing loss of function of *Tgfβr2* have low basal expression of *Serpin1* and are not Tgfβ responsive (Supplementary Figure 3). Next, removal of Wnt-ligands, Wnt3a and Rspo2, kills WT, $Braf^{V600E}$, $Braf^{V600E}\Delta T$ and control transfected cultures (Figure 2B). However, transfection of plasmids encoding Cas9 and guideRNAs (gRNAs) targeting the negative Wnt regulators, *Rnf43* and *Znrf3*, allowed outgrowth of organoids with cystic morphology (Figure 2B, growth of organoids in Wnt-ligand deficient NT medium). Loss of the p16Ink4a tumour suppressor was not directly selected for using changed media conditions, but this gene was targeted simultaneously with *Rnf43* and *Znrf3* and its loss likely provided a growth advantage to $Braf^{V600E}$ mutant cells [17]. This resulted in $Braf^{V600E}$;$Tgfbr2^{\Delta/\Delta}$;$Rnf43^{\Delta/\Delta}/Znrf3^{\Delta/\Delta}$;$p16\ Ink4a^{\Delta/\Delta}$ ($Braf^{V600E}\Delta TRZI$) organoids. qRT-PCR analysis of the Wnt-pathway response genes, *Axin2* and *Lgr5*, showed that activation of this pathway in the $Braf^{V600E}\Delta TRZI$ organoids in the absence of Wnt ligands is similar to the level in control $Braf^{V600E}$ organoids cultured in the presence of Wnt ligands, i.e. the pathway is super-activated by targeting *Rnf43* and *Znrf3*

(Supplementary Figure 3). qRT-PCR analysis also indicates a reduction in p16Ink4a mRNA levels in *Braf*^{V600E}Δ*TRZI* compared to *Braf*^{V600E} organoids (Supplementary Figure 3).

Lastly, to select for loss of *Mlh1* we exploited the clinical finding that MSI-High (MSI-H) cancers are reported to show relative resistance to the chemotherapeutic 5-fluorouracil (5-FU) [33]. We used media containing 5-FU to promote DNA mismatches [34]. Mlh1 is an essential component of the DNA mismatch machinery [35] and so we hypothesised that inactivation of *Mlh1* would lead to increased survival of cells despite DNA damage-arrest signals, consistent with the poor response of MSI CRC to 5-FU based adjuvant chemotherapy [33]. Organoids that had been transfected with a plasmid encoding Cas9 and a gRNA targeting *Mlh1* (*Braf*^{V600E}Δ*TRZIM*) were better able to withstand a pulse of 5FU treatment than control transfected *Braf*^{V600E}Δ*TRZI* (Figure 2B). The activity of previously unpublished gRNAs (*Tgfβr2* and *Mlh1* gRNAs) was evaluated in polyclonal organoids before proceeding to handpicking single clones and expansion of lines (Supplementary Figure 4). We also used bioinformatic prediction of the possible off-target sites for each of these gRNAs and verified that they were not changed in our organoid lines by Sanger sequencing (Supplementary Table 1). Bi-allelic, loss of function insertions and deletions (indels) in target genes were verified using DNA sequencing (Figure 2C, Supplementary Table 2).

To assess the effect of this series of genetic alterations on colorectal tumourigenesis, we transplanted organoids into NOD.Cg-*Prkdc*^{scid}*Il2rg*$^{tm1Wjl/Szj}$ (NSG) mice and used *in vivo* murine colonoscopy to directly visualize and score pathologic changes (Figure 3A, Supplementary Videos). Using a modified needle attachment, we injected organoids into the orthotopic site, the mucosal layer of the colon wall (Figure 3A, Supplementary Figure 5A, 5B) [36]. Injection of *Braf*^{V600E} mutant organoids failed to induce tumour formation over a 3 month time course as assessed by colonoscopic surveillance, at necropsy and by pathological evaluation (Figure 3B, 4B, Supplementary Figure 6). Introduction of Tgfβ pathway perturbation in *Braf*^{V600E}Δ*T* organoids results in 57% of organoid injections forming tumours within 3 months (Figure 3B). However, significantly more *Braf*^{V600E}Δ*TRZI* and *Braf*^{V600E}Δ*TRZIM* injected organoids formed tumours, 98% and 100% respectively (Figure 3B, $p<0.05$). Similar to human sessile serrated polyps, 94% (n=11 mice) of *Braf*^{V600E}Δ*TRZI* and 100% (n=8 mice) of *Braf*^{V600E}Δ*TRZIM* tumours developed a noticeable mucus cap visible from two weeks post-injection via colonoscopic surveillance [37] (Supplementary Figure 5C). This is in contrast to only 9% (n=12 mice) of the *Braf*^{V600E}Δ*T* tumours with a mucus cap. The more genetically complex organoids (*Braf*^{V600E}Δ*TRZI* and *Braf*^{V600E}Δ*TRZIM*) grew significantly more quickly than *Braf*^{V600E}Δ*T* tumours (Figure 3C, Supplementary Figure 6, $p<0.001$) and overall survival was also significantly decreased, with mean time from injection to humane endpoint of the experiment at 6 weeks for *Braf*^{V600E}Δ*TRZI* and 4 weeks for *Braf*^{V600E}Δ*TRZIM* (Figure 3D, $p<0.001$).

Histologically, tumours generated using *Braf*^{V600E}Δ*T*, *Braf*^{V600E}Δ*TRZI* and *Braf*^{V600E}Δ*TRZIM* organoids are invasive, adenocarcinomas with features of human serrated CRC (Figure 4, Supplementary Table 3) [2, 38]. We observed infrequent liver metastasis (9% or 1 out of 11) mice), with no macro-metastasis to other sites (lung,

peritoneum) after injection with *Braf*^{V600E}Δ*TRZI* (Supplementary Figure 5D). Organoid-derived cells were readily visualised by morphology and using immunohistochemical detection of Braf^{V600E} (Figure 4D, Supplementary Figure 5E). The tumours display a substantial desmoplastic stromal reaction (Figure 4E), particularly with *Braf*^{V600E}Δ*TRZI* compared to the less genetically complex *Braf*^{V600E}Δ*T* (85% vs. 33% $p<0.05$, Supplementary Table 3). Thus the genetics of the tumour in this model was important in the co-evolution of the stroma. This stromal reaction is composed of smooth muscle actin expressing cancer activated fibroblasts amongst other cell types (Figure 4G). The more complex *Braf*^{V600E}Δ*TRZI* and *Braf*^{V600E}Δ*TRZIM,* but not *Braf*^{V600E}Δ*T* tumours, featured tumour budding (Figure 4F, Supplementary Figure 5F) and approximately half were categorised as mucinous adenocarcinoma [38], indicating a change to the amount of mucin produced by tumours with more complex genetic alterations, (42–50% vs. 0% $p<0.01$, Supplementary Table 3). This could also be visualised using Alcian Blue mucin staining (Figure 4G). *Muc2* mRNA, encoding a core component of mucus, was increased in the *Braf*^{V600E}Δ*TRZI* but not the *Braf*^{V600E} or *Braf*^{V600E}Δ*T* organoids ($p<0.05$, Supplementary Figure 7).

To investigate the consequences of mutating the essential DNA damage response gene, *Mlh1*, we analysed microsatellite marker length in our organoid series. *Braf*^{V600E}Δ*TRZIM,* but not *Braf*^{V600E}Δ*TRZI* organoids have altered microsatellite length (MSI) when compared to the donor mouse from which organoids were derived, in 4 mononucleotide markers previously validated for use in mouse [39, 40]. These cells accrued further MSI *in vivo*, with *Braf*^{V600E}Δ*TRZIM*, but not *Braf*^{V600E}Δ*TRZI* tumours containing additional microsatellite tract length variability (Supplementary Figure 8).

Discrete transcript profiles of serrated and conventional pathway tumours

In addition to our series of serrated pathway tumours, we also generated tumours driven by alteration of commonly mutated conventional CRC pathway genes, *Apc* and *Kras*^{G12D}. Similar to previous reports [36], colonic organoids expressing adeno-virally delivered Cre, derived from *Kras*$^{LSL\text{-}G12D/+}$;*Apc*$^{fl/fl}$ mice survived culture in the absence of Wnt3a or Rspo2 (Supplementary Figure 9). Adenocarcinomas arising from orthotopic injection of *Kras*$^{G12D/+}$;*Apc*$^{fl/fl}$ organoids, were verified as *Kras*$^{G12D/+}$;*Apc*$^{\Delta 580l/\Delta 580}$ (*Kras*^{G12D};*Apc*$^{\Delta/\Delta}$) genotype and displayed nuclear β-catenin localisation (Supplementary Figure 9). We isolated RNA from our series of serrated and conventional pathway tumours and compared mRNAseq expression profiles between these different tumours and normal colonic mucosa from tumour bearing animals (n=4 biological replicates per group). The multidimensional scaling (MDS) plot generated from our RNAseq data showed that, as expected, the normal colon samples had quite different transcript profiles to the tumour samples (Figure 5A). In comparison, the *Braf*^{V600E}, serrated subtype tumours all clustered closely together and separated from the *Kras*^{G12D};*Apc*$^{\Delta/\Delta}$ tumours (Figure 5A). Consistent with alterations to the MAPK pathway in our *Braf*^{V600E} organoid series, gene set enrichment analysis (GSEA) identified differential expression of MAPK-pathway transcripts as enriched in the *Braf*^{V600E} tumours compared to normal colon (Supplementary Figure 10A). Validating our attempt to model MSI CRC, the tumours derived from *Braf*^{V600E}Δ*TRZIM* organoids were also

significantly enriched for differential expression of a human MSI CRC-associated gene set (Supplementary Figure 10B) [41].

The top enriched gene set based on normalised enrichment score in our analyses across all $Braf^{V600E}$, but not $Kras^{G12D};Apc^{\Delta/\Delta}$, tumours when compared to normal colon was the sphingolipid (SP) *de novo* biosynthesis pathway (Figure 5B, Supplementary Table 4). We validated the differential expression of SP pathway transcripts from the leading edge of the GSEA by real-time qPCR in $Braf^{V600E}$ and conventional pathway tumours (Figure 5C, Supplementary Figure 11). Two key enzymes regulating S1P levels in this pathway are sphingosine kinase 1 (SPHK1) and the counter-acting sphingosine-1-phosphate phosphatase 1 (SGPP1) [42]. Consistent with previous reports in human CRC [43, 44], we observed increased expression of *Sphk1* transcripts in our series of $Braf^{V600E}$ tumours compared to normal mouse colon and a converse decrease in *Sgpp1* transcripts (Figure 5C). This suggested at the transcriptomic level that the pathway may be primed for increased production of the pro-survival molecule sphingosine 1-phosphate (S1P) in our model of serrated CRC [42]. We next wished to determine if this shift at the transcript level was also observed in human CRC samples. *SPHK1* was significantly upregulated in 622 TCGA CRC samples compared to matched normal controls, with greatest expression levels in $BRAF^{V600E}$ tumours (Figure 5D). Conversely, *SGPP1* expression was significantly decreased in all CRC samples compared to matched normal controls. Increased expression of *SPHK1* and decreased expression of *SGPP1* were both separately associated with poor survival in the TCGA cohort (Figure 5E).

DISCUSSION

Here we have focused on the serrated pathway to CRC that accounts for up to 25% of all CRC, and for microsatellite stable cases has very poor outcome [2]. We have developed a panel of CRISPR/Cas9 genome engineered organoids that model DNA alterations found in *BRAF* mutant serrated CRC. In this way we are producing novel, preclinical models of colorectal adenocarcinoma with features of serrated CRC, and most notably desmoplastic stromal responses, infiltrative growth, tumour budding and mucinous differentiation [2, 45, 46] (**see** Figure 4, Supplementary Table 3 & Figure 5). Mucous caps characterise human serrated polyps at colonoscopy. When we look at an early time point in tumour development in our serrated CRC mouse models with complex genetics ($Braf^{V600E}\Delta TRZI$ and $Braf^{V600E}\Delta TRZIM$) we also observe mucous caps. Previous studies using CRISPR/Cas9 to model the conventional molecular pathway to CRC using human intestinal organoids were either unable to generate invasive CRC [12], or required 4 gene alterations for invasive tumour growth [13]. We find here that alterations to just two genes, *Braf* and *Tgfbr2*, results in transmurally invasive adenocarcinoma. Further altering the oncogene-induced senescence factor, *p16 Ink4a*, and the Wnt pathway leads to increased tumour initiation and decreased survival time (Figure 3 & 4). These more genetically complex tumours had increased stromal response, tumour budding and mucinous differentiation. We also model MSI "hypermutator" CRC by inducing loss-of-function mutations in the DNA mismatch repair gene, *Mlh1*. Similar to recent work describing a 6-fold higher DNA mutation rate in CRISPR/Cas9 engineered $MLH1^{\Delta/\Delta}$ human colon organoid lines [47], we have successfully

generated the MSI phenotype as judged by instability in microsatellite repeat tract length (Supplementary Figure 8).

We utilise the recently adapted small animal colonoscopy technique [36, 48] to enable rapid, orthotopic injection of engineered organoids to the mucosal layer of the colon wall and tumour monitoring thereafter (Supplementary Figure 5 & videos). This is especially salient given the observed differences in metastatic potential for engineered conventional pathway CRC organoids delivered either subcutaneously or using a rectal prolapse model, where only tumours growing at the orthotopic colon site produced liver metastases [49]. A second report using similar conventional pathway mutant organoids injected using a colonoscope resulted in metastasis in 30% of mice [36]. We observe liver metastasis in the serrated CRC models presented here, albeit infrequently, and no lung or peritoneal spread of the disease. This may be due to the model not containing strong metastasis promoting alterations or alternately, in the future, luminal preservation through colonoscopic biopsy may allow a more complete evaluation of disease progression.

These models will advance this field by providing a rapid, inexpensive and pathologically faithful approach to studying the biology of serrated CRC. Other models, whilst valuable in their own right, are slow, require complicated *in vivo* breeding and have a prescribed number and sequence of genetic alterations [18, 19, 50, 51, 52, 53]. Our models can be readily adapted to investigate the many leads generated by next generation sequencing of human serrated CRC and will be particularly valuable for testing potential therapeutics in the setting of complex, but known, genetic landscapes. Transcriptome analysis of our genome engineered models of serrated and conventional CRC have identified putative changes to sphingolipid metabolism in these tumours. The differential expression of transcripts encoding two key enzymes in this pathway are mirrored in human CRC and are associated with worse prognosis. Future work will investigate the therapeutic efficacy of targeting the sphingolipid biosynthesis pathway for $BRAF^{V600E}$ CRC.

METHODS

Mouse experiments

This study was approved by the MIT Institutional Animal Care and Use Committee, QIMR Berghofer and SAHMRI Animal Ethics committees (P1208, SAM174, SAM205). Mice heterozygous for both the conditionally active $Braf^{CA}$ and $Villin\text{-}Cre^{ERT2}$ alleles to induce the mutation analogous to human $BRAF^{V600E}$ specifically in the intestine were generated as described [52]. Similarly, mice containing the $Kras^{LSL\text{-}G12D/+}$ [54] and $Apc^{CKO/CKO}$ [55] alleles were interbred to produce double transgenic offspring that were used to generate $Kras^{G12D/+}$; $Apc^{\Delta 580l/\Delta 580}$ colonic organoids [36].

Orthotopic Injection

NOD.Cg-$Prkdc^{scid}Il2rg^{tm1Wjl}$/SzJ (NSG) mice (male and female, 6–12 weeks old) were obtained from the SAHMRI Bioresources facility and housed under pathogen-free conditions. Organoids were isolated from matrigel and dissociated to single cells and small clusters using TrypLE. The cell clusters (equivalent to ~150 organoids) were washed three

times with cold PBS containing 10uM Y-27632 and then resuspended in 20ul 10% GFR matrigel 1:1000 india ink, 10uM Y-27632 in PBS and injected into the mucosa of the distal colon of anaesthetised NSG mice. Colonoscopy-guided orthotopic injection into the colon wall was undertaken as previously described [36] with modifications described in Supplementary methods.

Genome engineering

gRNAs specific for each target gene were either published sequences targeting *Rnf43, Znrf3* or *p16 Ink4a* [56, 57] or designed *de novo* using the CRISPR design Tool to target the first exon immediately downstream of the translation start codon [11] (see Supplementary Methods table 2). gRNA oligos were cloned into px-459, which expresses both the Cas9 nuclease and single gRNAs [11]. Organoid transfection and culture details are included in the Supplementary methods section.

Nucleic acid analyses, bioinformatics, western blotting and immunohistochemistry

Please see the Supplementary Methods section.

Supplementary Material

Refer to Web version on PubMed Central for supplementary material.

Acknowledgments

The Rspo-2 expression plasmid was a kind gift from Prof. Antony Burgess (Walter & Eliza Hall Institute of Medical Research, Australia), L-Wnt3a cells were a kind gift of Prof. Hans Clevers (Hubrecht Institute, The Netherlands). Dr. Mark Van der Hoek and staff at the David R. Gunn Genomics Facility at SAHMRI, John Toubia, Andreas Schreiber, Joel Geoghegan and staff at the Adelaide Australian Cancer Research Foundation Genomics Facility for useful discussions.

This work was supported by Cure Cancer Australia/Cancer Australia (APP1102534), the Cancer Council SA Beat Cancer Project on behalf of its donors and the State Government of South Australia through the Department of Health SA, by Pathology Queensland, by the Australian National Health and Medical Research Council (NHMRC) through (APP1081852, APP1140236), by the National Institutes of Health (NIH) (K08 CA198002, R00 AG045144, R01 CA211184), the Department of Defense (CA120198), the V Foundation V Scholar Award, the Sidney Kimmel Scholar Award, the Pew-Stewart Trust Scholar Award, the Koch Institute Frontier Research Program through the Kathy and Curt Marble Cancer Research Fund, the American Federation of Aging Research, as well as by the Koch Institute Support Grant P30-CA14051 from the National Cancer Institute. DLW is supported by a NHMRC Career Development Fellowship, VLW by a Gastroenterological Society of Australia Senior Research Fellowship.

Abbreviations

CRC	colorectal cancer
MAPK	mitogen activated kinase
CIMP	CpG Island Methylator Phenotype
CIN	chromosomal instability
APC	*Adenomatous polyposis coli*
EGF	Epidermal growth factor

BMP	bone morphogenic protein
TCGA	The Cancer Genome Atlas
MSI	microsatellite instability
TGFβ	transforming growth factor-β
MLH1	*MutL homolog 1*
4-OHT	4-hydroxytamoxifen
EGFR	epidermal growth factor receptor
CRISPR	clustered regularly interspaced short palindromic repeats
WT	wild type
qRT-PCR	Quantitative real-time PCR
gRNAs	guideRNAs
MSI-H	MSI-High
NSG	NOD.Cg-*Prkdc*^{scid}*Il2rg*$^{tm1Wjl/Szj}$
MDS	multidimensional scaling
GSEA	gene set enrichment analysis
SP	sphingolipid
SPHK1	sphingosine kinase 1
SGPP1	sphingosine-1-phosphate phosphatase 1
S1P	sphingosine 1-phosphate
Braf*^{V600E}*ΔT	*Braf*^{V600E}*Tgfbr2*$^{Δ/Δ}$
Braf*^{V600E}*ΔTRZI	*Braf*^{V600E} *Tgfbr2*$^{Δ/Δ}$ *Rnf43*$^{Δ/Δ}$*/Znrf3*$^{Δ/Δ}$ *p16Ink4a*$^{Δ/Δ}$
Braf*^{V600E} *ΔTRZIM	*Braf*^{V600E} *Tgfbr2*$^{Δ/Δ}$*Rnf43*$^{Δ/Δ}$*/Znrf3*$^{Δ/Δ}$ *p16Ink4a*$^{Δ/Δ}$*Mlh1*$^{Δ/Δ}$
W	Wnt-3a
R	Rspo-2
N	Noggin
T	TGFβ1
5FU	5-Fluorouracil
ES	Enrichment score

NES	normalised enrichment score
FDR	false discovery rate

References

1. Fearon ER, Vogelstein B. A genetic model for colorectal tumorigenesis. Cell. 1990; 61:759–67. [PubMed: 2188735]
2. Bettington M, Walker N, Clouston A, Brown I, Leggett B, Whitehall V. The serrated pathway to colorectal carcinoma: current concepts and challenges. Histopathology. 2013; 62:367–86. [PubMed: 23339363]
3. Weisenberger DJ, Siegmund KD, Campan M, Young J, Long TI, Faasse MA, et al. CpG island methylator phenotype underlies sporadic microsatellite instability and is tightly associated with BRAF mutation in colorectal cancer. Nature genetics. 2006; 38:787–93. [PubMed: 16804544]
4. Tejpar S, Bertagnolli M, Bosman F, Lenz HJ, Garraway L, Waldman F, et al. Prognostic and predictive biomarkers in resected colon cancer: current status and future perspectives for integrating genomics into biomarker discovery. Oncologist. 2010; 15:390–404. [PubMed: 20350999]
5. Pai RK, Jayachandran P, Koong AC, Chang DT, Kwok S, Ma L, et al. BRAF-mutated, microsatellite-stable adenocarcinoma of the proximal colon: an aggressive adenocarcinoma with poor survival, mucinous differentiation, and adverse morphologic features. Am J Surg Pathol. 2012; 36:744–52. [PubMed: 22314188]
6. Rex DK, Ahnen DJ, Baron JA, Batts KP, Burke CA, Burt RW, et al. Serrated lesions of the colorectum: review and recommendations from an expert panel. Am J Gastroenterol. 2012; 107:1315–29. [PubMed: 22710576]
7. Anderson JC, Robertson DJ. Serrated Polyp Detection by the Fecal Immunochemical Test: An Imperfect FIT. Clinical gastroenterology and hepatology : the official clinical practice journal of the American Gastroenterological Association. 2017; 15:880–2. [PubMed: 27847280]
8. Sato T, Stange DE, Ferrante M, Vries RG, Van Es JH, Van den Brink S, et al. Long-term expansion of epithelial organoids from human colon, adenoma, adenocarcinoma, and Barrett's epithelium. Gastroenterology. 2011; 141:1762–72. [PubMed: 21889923]
9. Barker N. Adult intestinal stem cells: critical drivers of epithelial homeostasis and regeneration. Nature reviews Molecular cell biology. 2014; 15:19–33. [PubMed: 24326621]
10. Clevers H. Modeling Development and Disease with Organoids. Cell. 2016; 165:1586–97. [PubMed: 27315476]
11. Ran FA, Hsu PD, Wright J, Agarwala V, Scott DA, Zhang F. Genome engineering using the CRISPR-Cas9 system. Nat Protoc. 2013; 8:2281–308. [PubMed: 24157548]
12. Matano M, Date S, Shimokawa M, Takano A, Fujii M, Ohta Y, et al. Modeling colorectal cancer using CRISPR-Cas9-mediated engineering of human intestinal organoids. Nat Med. 2015; 21:256–62. [PubMed: 25706875]
13. Drost J, van Jaarsveld RH, Ponsioen B, Zimberlin C, van Boxtel R, Buijs A, et al. Sequential cancer mutations in cultured human intestinal stem cells. Nature. 2015; 521:43–7. [PubMed: 25924068]
14. Fujii M, Shimokawa M, Date S, Takano A, Matano M, Nanki K, et al. A Colorectal Tumor Organoid Library Demonstrates Progressive Loss of Niche Factor Requirements during Tumorigenesis. Cell Stem Cell. 2016; 18:827–38. [PubMed: 27212702]
15. Cancer Genome Atlas N. Comprehensive molecular characterization of human colon and rectal cancer. Nature. 2012; 487:330–7. [PubMed: 22810696]
16. Cohen R, Cervera P, Svrcek M, Pellat A, Dreyer C, de Gramont A, et al. BRAF-Mutated Colorectal Cancer: What Is the Optimal Strategy for Treatment? Curr Treat Options Oncol. 2017; 18:9. [PubMed: 28214977]
17. Kriegl L, Neumann J, Vieth M, Greten FR, Reu S, Jung A, et al. Up and downregulation of p16(Ink4a) expression in BRAF-mutated polyps/adenomas indicates a senescence barrier in the serrated route to colon cancer. Modern pathology : an official journal of the United States and Canadian Academy of Pathology, Inc. 2011; 24:1015–22.

18. Bennecke M, Kriegl L, Bajbouj M, Retzlaff K, Robine S, Jung A, et al. Ink4a/Arf and oncogene-induced senescence prevent tumor progression during alternative colorectal tumorigenesis. Cancer Cell. 2010; 18:135–46. [PubMed: 20708155]
19. Rad R, Cadinanos J, Rad L, Varela I, Strong A, Kriegl L, et al. A genetic progression model of Braf(V600E)-induced intestinal tumorigenesis reveals targets for therapeutic intervention. Cancer Cell. 2013; 24:15–29. [PubMed: 23845441]
20. Krtolica K, Krajnovic M, Usaj-Knezevic S, Babic D, Jovanovic D, Dimitrijevic B. Comethylation of p16 and MGMT genes in colorectal carcinoma: correlation with clinicopathological features and prognostic value. World J Gastroenterol. 2007; 13:1187–94. [PubMed: 17451198]
21. Ma X, Wang YW, Zhang MQ, Gazdar AF. DNA methylation data analysis and its application to cancer research. Epigenomics. 2013; 5:301–16. [PubMed: 23750645]
22. Herman JG, Merlo A, Mao L, Lapidus RG, Issa JP, Davidson NE, et al. Inactivation of the CDKN2/p16/MTS1 gene is frequently associated with aberrant DNA methylation in all common human cancers. Cancer Res. 1995; 55:4525–30. [PubMed: 7553621]
23. Bond CE, McKeone DM, Kalimutho M, Bettington ML, Pearson SA, Dumenil TD, et al. RNF43 and ZNRF3 are commonly altered in serrated pathway colorectal tumorigenesis. Oncotarget. 2016; 7:70589–600. [PubMed: 27661107]
24. Koo BK, Spit M, Jordens I, Low TY, Stange DE, van de Wetering M, et al. Tumour suppressor RNF43 is a stem-cell E3 ligase that induces endocytosis of Wnt receptors. Nature. 2012; 488:665–9. [PubMed: 22895187]
25. Murakami T, Mitomi H, Saito T, Takahashi M, Sakamoto N, Fukui N, et al. Distinct WNT/beta-catenin signaling activation in the serrated neoplasia pathway and the adenoma-carcinoma sequence of the colorectum. Modern pathology : an official journal of the United States and Canadian Academy of Pathology, Inc. 2015; 28:146–58.
26. Borowsky J, Dumenil T, Bettington M, Pearson SA, Bond C, Fennell L, et al. The role of APC in WNT pathway activation in serrated neoplasia. Modern pathology : an official journal of the United States and Canadian Academy of Pathology, Inc. 2017
27. Giannakis M, Hodis E, Jasmine Mu X, Yamauchi M, Rosenbluh J, Cibulskis K, et al. RNF43 is frequently mutated in colorectal and endometrial cancers. Nature genetics. 2014; 46:1264–6. [PubMed: 25344691]
28. Parsons R, Myeroff LL, Liu B, Willson JK, Markowitz SD, Kinzler KW, et al. Microsatellite instability and mutations of the transforming growth factor beta type II receptor gene in colorectal cancer. Cancer research. 1995; 55:5548. [PubMed: 7585632]
29. Li X, Yao X, Wang Y, Hu F, Wang F, Jiang L, et al. MLH1 promoter methylation frequency in colorectal cancer patients and related clinicopathological and molecular features. PLoS One. 2013; 8:e59064. [PubMed: 23555617]
30. IJspeert J, Vermeulen L, Meijer GA, Dekker E. Serrated neoplasia-role in colorectal carcinogenesis and clinical implications. Nat Rev Gastroenterol Hepatol. 2015; 12:401–9. [PubMed: 25963511]
31. Di Nicolantonio F, Martini M, Molinari F, Sartore-Bianchi A, Arena S, Saletti P, et al. Wild-type BRAF is required for response to panitumumab or cetuximab in metastatic colorectal cancer. Journal of clinical oncology : official journal of the American Society of Clinical Oncology. 2008; 26:5705–12. [PubMed: 19001320]
32. Fessler E, Drost J, van Hooff SR, Linnekamp JF, Wang X, Jansen M, et al. TGFbeta signaling directs serrated adenomas to the mesenchymal colorectal cancer subtype. EMBO Mol Med. 2016; 8:745–60. [PubMed: 27221051]
33. Ribic CM, Sargent DJ, Moore MJ, Thibodeau SN, French AJ, Goldberg RM, et al. Tumor Microsatellite-Instability Status as a Predictor of Benefit from Fluorouracil-Based Adjuvant Chemotherapy for Colon Cancer. New England Journal of Medicine. 2003; 349:247–57. [PubMed: 12867608]
34. Longley DB, Harkin DP, Johnston PG. 5-fluorouracil: mechanisms of action and clinical strategies. Nat Rev Cancer. 2003; 3:330–8. [PubMed: 12724731]
35. Li GM. Mechanisms and functions of DNA mismatch repair. Cell Res. 2008; 18:85–98. [PubMed: 18157157]

36. Roper J, Tammela T, Cetinbas NM, Akkad A, Roghanian A, Rickelt S, et al. In vivo genome editing and organoid transplantation models of colorectal cancer and metastasis. Nat Biotechnol. 2017; 35:569–76. [PubMed: 28459449]
37. Saito S, Tajiri H, Ikegami M. Serrated polyps of the colon and rectum: Endoscopic features including image enhanced endoscopy. World J Gastrointest Endosc. 2015; 7:860–71. [PubMed: 26240687]
38. Bosman FT, Carneiro F, Hruban RH, Theise ND. WHO Classification of Tumours of the Digestive System. 2010
39. Bacher JW, Abdel Megid WM, Kent-First MG, Halberg RB. Use of mononucleotide repeat markers for detection of microsatellite instability in mouse tumors. Mol Carcinog. 2005; 44:285–92. [PubMed: 16240453]
40. Kabbarah O, Mallon MA, Pfeifer JD, Edelmann W, Kucherlapati R, Goodfellow PJ. A panel of repeat markers for detection of microsatellite instability in murine tumors. Mol Carcinog. 2003; 38:155–9. [PubMed: 14639654]
41. Watanabe T, Kobunai T, Toda E, Yamamoto Y, Kanazawa T, Kazama Y, et al. Distal colorectal cancers with microsatellite instability (MSI) display distinct gene expression profiles that are different from proximal MSI cancers. Cancer Res. 2006; 66:9804–8. [PubMed: 17047040]
42. Pitson SM. Regulation of sphingosine kinase and sphingolipid signaling. Trends Biochem Sci. 2011; 36:97–107. [PubMed: 20870412]
43. Kawamori T, Osta W, Johnson KR, Pettus BJ, Bielawski J, Tanaka T, et al. Sphingosine kinase 1 is up-regulated in colon carcinogenesis. FASEB J. 2006; 20:386–8. [PubMed: 16319132]
44. Oskouian B, Saba J. Sphingosine-1-phosphate metabolism and intestinal tumorigenesis: lipid signaling strikes again. Cell Cycle. 2007; 6:522–7. [PubMed: 17361098]
45. Chen D, Huang JF, Liu K, Zhang LQ, Yang Z, Chuai ZR, et al. BRAFV600E mutation and its association with clinicopathological features of colorectal cancer: a systematic review and meta-analysis. PLoS One. 2014; 9:e90607. [PubMed: 24594804]
46. Garcia-Solano J, Conesa-Zamora P, Trujillo-Santos J, Makinen MJ, Perez-Guillermo M. Tumour budding and other prognostic pathological features at invasive margins in serrated colorectal adenocarcinoma: a comparative study with conventional carcinoma. Histopathology. 2011; 59:1046–56. [PubMed: 22175885]
47. Drost J, van Boxtel R, Blokzijl F, Mizutani T, Sasaki N, Sasselli V, et al. Use of CRISPR-modified human stem cell organoids to study the origin of mutational signatures in cancer. Science. 2017; 358:234–8. [PubMed: 28912133]
48. Zigmond E, Halpern Z, Elinav E, Brazowski E, Jung S, Varol C. Utilization of murine colonoscopy for orthotopic implantation of colorectal cancer. PLoS One. 2011; 6:e28858. [PubMed: 22174916]
49. de Sousa e Melo F, Kurtova AV, Harnoss JM, Kljavin N, Hoeck JD, Hung J, et al. A distinct role for Lgr5(+) stem cells in primary and metastatic colon cancer. Nature. 2017; 543:676–80. [PubMed: 28358093]
50. Carragher LA, Snell KR, Giblett SM, Aldridge VS, Patel B, Cook SJ, et al. V600EBraf induces gastrointestinal crypt senescence and promotes tumour progression through enhanced CpG methylation of p16INK4a. EMBO molecular medicine. 2010; 2:458–71. [PubMed: 20941790]
51. Davies EJ, Marsh Durban V, Meniel V, Williams GT, Clarke AR. PTEN loss and KRAS activation leads to the formation of serrated adenomas and metastatic carcinoma in the mouse intestine. The Journal of pathology. 2014; 233:27–38. [PubMed: 24293351]
52. Bond CE, Liu C, Kawamata F, McKeone DM, Fernando W, Jamieson S, et al. Oncogenic BRAF mutation induces DNA methylation changes in a murine model for human serrated colorectal neoplasia. Epigenetics. 2017:01–20.
53. Coffee EM, Faber AC, Roper J, Sinnamon MJ, Goel G, Keung L, et al. Concomitant BRAF and PI3K/mTOR blockade is required for effective treatment of BRAF(V600E) colorectal cancer. Clinical cancer research : an official journal of the American Association for Cancer Research. 2013; 19:2688–98. [PubMed: 23549875]
54. Jackson EL, Willis N, Mercer K, Bronson RT, Crowley D, Montoya R, et al. Analysis of lung tumor initiation and progression using conditional expression of oncogenic K-ras. Genes Dev. 2001; 15:3243–8. [PubMed: 11751630]

55. Kuraguchi M, Wang XP, Bronson RT, Rothenberg R, Ohene-Baah NY, Lund JJ, et al. Adenomatous polyposis coli (APC) is required for normal development of skin and thymus. PLoS Genet. 2006; 2:e146. [PubMed: 17002498]

56. Schwank G, Koo BK, Sasselli V, Dekkers JF, Heo I, Demircan T, et al. Functional repair of CFTR by CRISPR/Cas9 in intestinal stem cell organoids of cystic fibrosis patients. Cell Stem Cell. 2013; 13:653–8. [PubMed: 24315439]

57. Chen S, Sanjana NE, Zheng K, Shalem O, Lee K, Shi X, et al. Genome-wide CRISPR screen in a mouse model of tumor growth and metastasis. Cell. 2015; 160:1246–60. [PubMed: 25748654]

SUMMARY BOX

What is already known about this subject

- 25% of colorectal cancers (CRC) form via an alternate molecular pathway typified by activating mutation in the BRAF kinase and accrual of epigenetic modifications at specific promoter locations.
- The molecular evolution of these serrated CRCs and how this relates to natural history is poorly understood and may hold the key to better treatment and prevention options for this form of CRC.

What are the new findings

- Here we use next generation sequence information from human serrated CRC, combined with organoid culture, gene editing and orthotopic transplantation techniques to rapidly generate complex, preclinical models of serrated CRC.

How might it impact on clinical practice in the foreseeable future?

- These preclinical models will allow therapeutic evaluation in known, previously untested genetic landscapes.
- Transcriptomic analysis of our models, combined with patient data, have suggested potential vulnerabilities for this tumour type that we will test in the future.

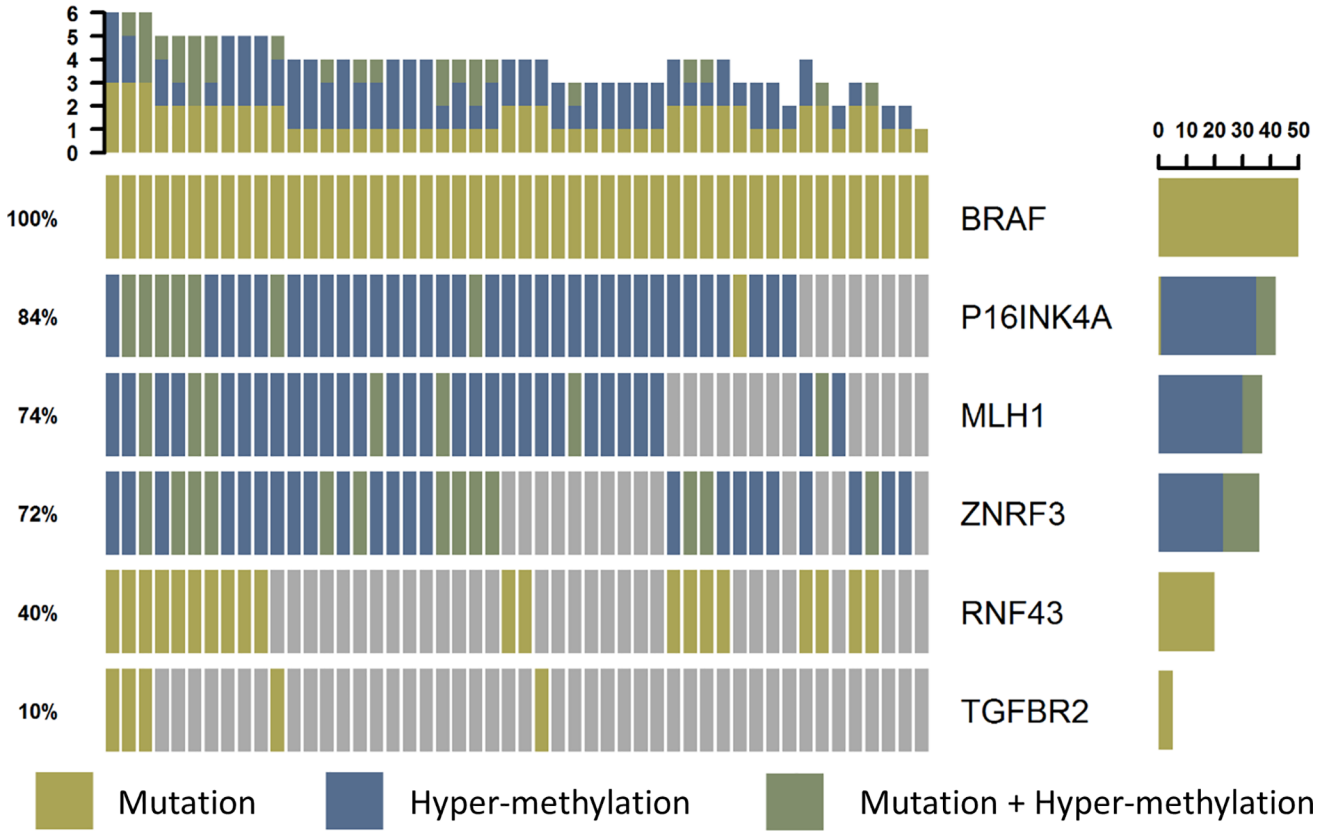

Figure 1. Co-occurring molecular events in stem-cell niche, microsatellite instability and senescence pathways in *BRAF*^{V600E} mutant serrated CRC

Of the 50 patients with *BRAF*^{V600E} CRC from the TCGA CRC cohort (n=527 patients total), we depict the co-alteration (non-synonymous mutation and/or hyper-methylation) of selected genes in these pathways. Number of patients with each alterations is indicated by bar graph on right, % of *BRAF*^{V600E} cases containing the alteration is indicated by numbers on left. Coloured blocks indicate gene is altered in the sample, grey is unaltered.

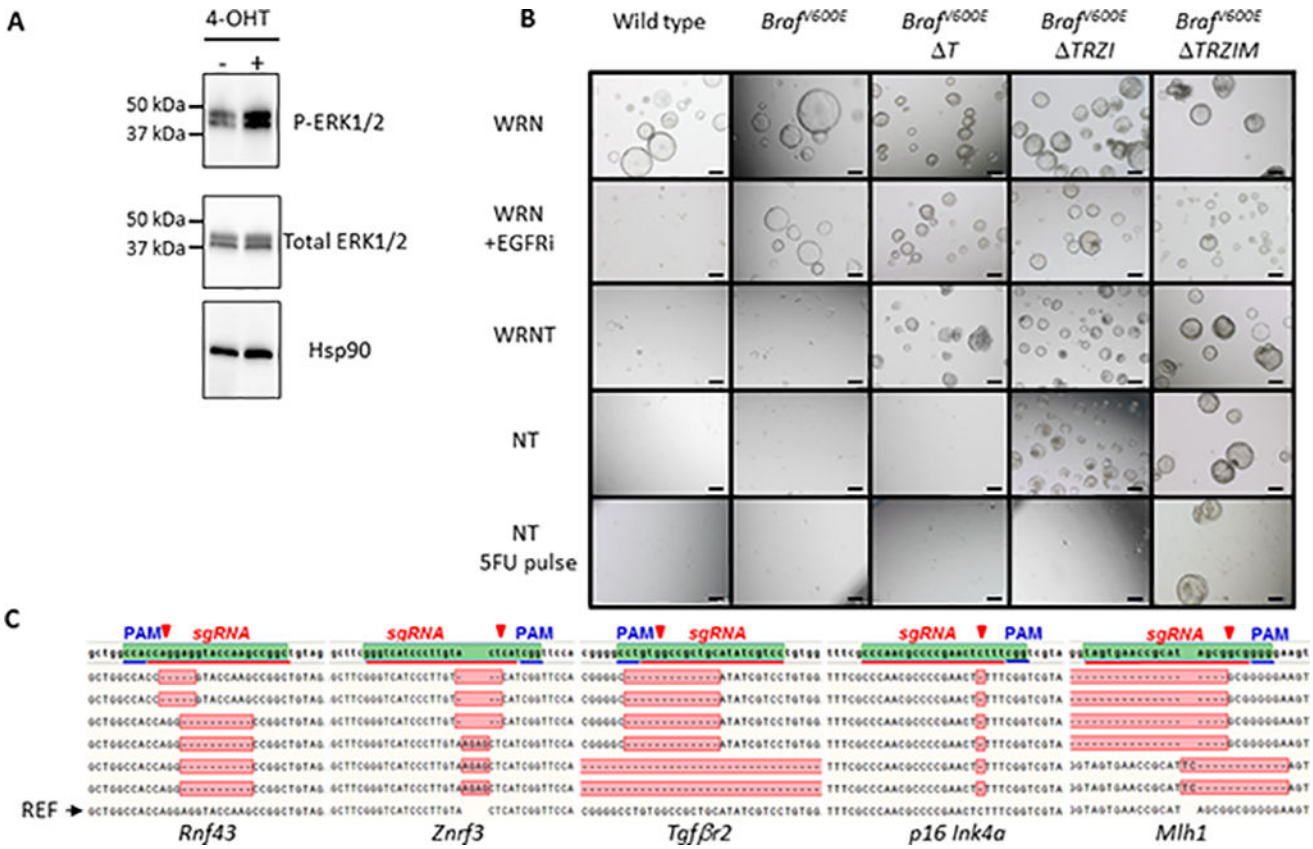

Figure 2. Introduction of genetic alterations associated with serrated CRC promotes independence from niche factor requirements

A, activation of MAPK pathway in *Braf*^{V600E} organoids visualized by phosphorylation of the ERK1/2 effector protein, 4-hydroxytamoxifen (4-OHT). **B,** Generation of a 'serratoid' series from normal mouse colonic organoids through sequential CRISPR/Cas9 targeting and *in vitro* selection. *Braf*^{V600E}, *Braf*^{V600E}*Tgfbr2*$^{\Delta/\Delta}$ (*Braf*^{V600E}*ΔT*), *Braf*^{V600E} *Tgfbr2*$^{\Delta/\Delta}$ *Rnf43*$^{\Delta/\Delta}$/*Znrf3*$^{\Delta/\Delta}$ *p16Ink4a*$^{\Delta/\Delta}$ (*Braf*^{V600E} *ΔTRZI*), *Braf*^{V600E} *Tgfbr2*$^{\Delta/\Delta}$*Rnf43*$^{\Delta/\Delta}$/*Znrf3*$^{\Delta/\Delta}$ *p16Ink4a*$^{\Delta/\Delta}$*Mlh1*$^{\Delta/\Delta}$ (*Braf*^{V600E} *ΔTRZIM).* Normal media components required as stem cell niche factors Wnt-3a (W), Rspo-2 (R), Noggin (N), additional selection with TGFβ1 (T) and chemotherapeutic agent, 5-Fluorouracil (5FU). **C,** DNA sequence verification of biallelic insertion/deletion (indel) mutations that result in prematurely truncated proteins.

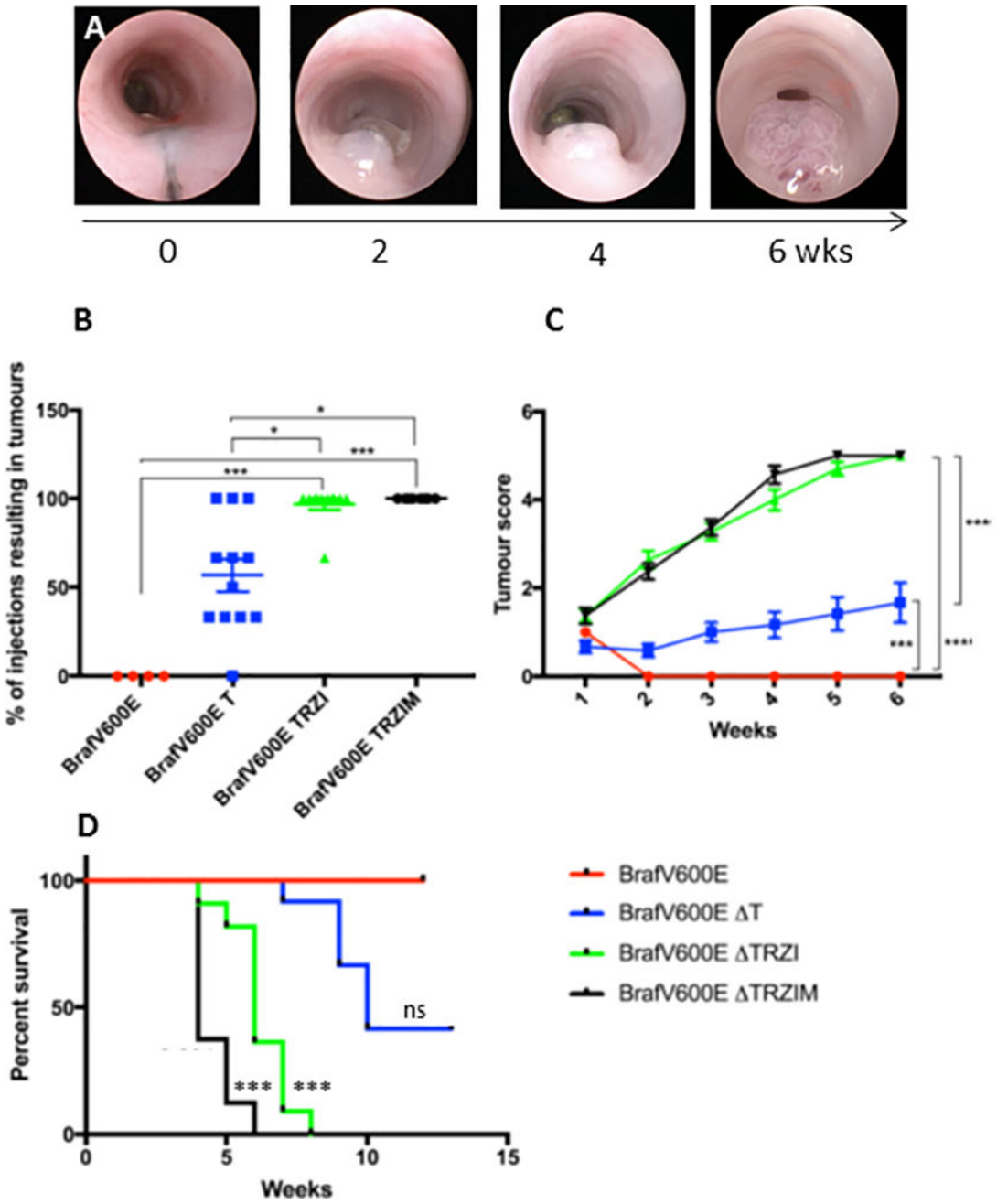

Figure 3. *Braf*^{V600E} alone is not sufficient for colon tumour formation, but with increasing serrated pathway genetic alterations tumour penetrance and growth rate increases

A, colonoscopic images showing injection and rapid growth of serratoid *Braf*^{V600E} *ΔTRZI* line. **B,** Tumour penetrance as a percentage of the number of organoid injections that gave rise to a tumour/mouse in 3 months for each line, with 1–3 injections/mouse. **C,** Colonoscopic scoring of largest tumour in each mouse (n=5 mice per group, Becker scale). **D,** Kaplan-Meier plot showing overall survival post-injection with organoid lines *Braf*^{V600E} n=4 mice, *Braf*^{V600E} *ΔT* n=12 mice, *Braf*^{V600E} *ΔTRZI* n=11 mice, *Braf*^{V600E} *ΔTRZIM* n=8

mice, compared to $Braf^{V600E}$ using a Bonferroni adjustment for multiple comparisons. ns=not significant, *=p≤0.05, **=p≤0.01, ***=p≤0.001.

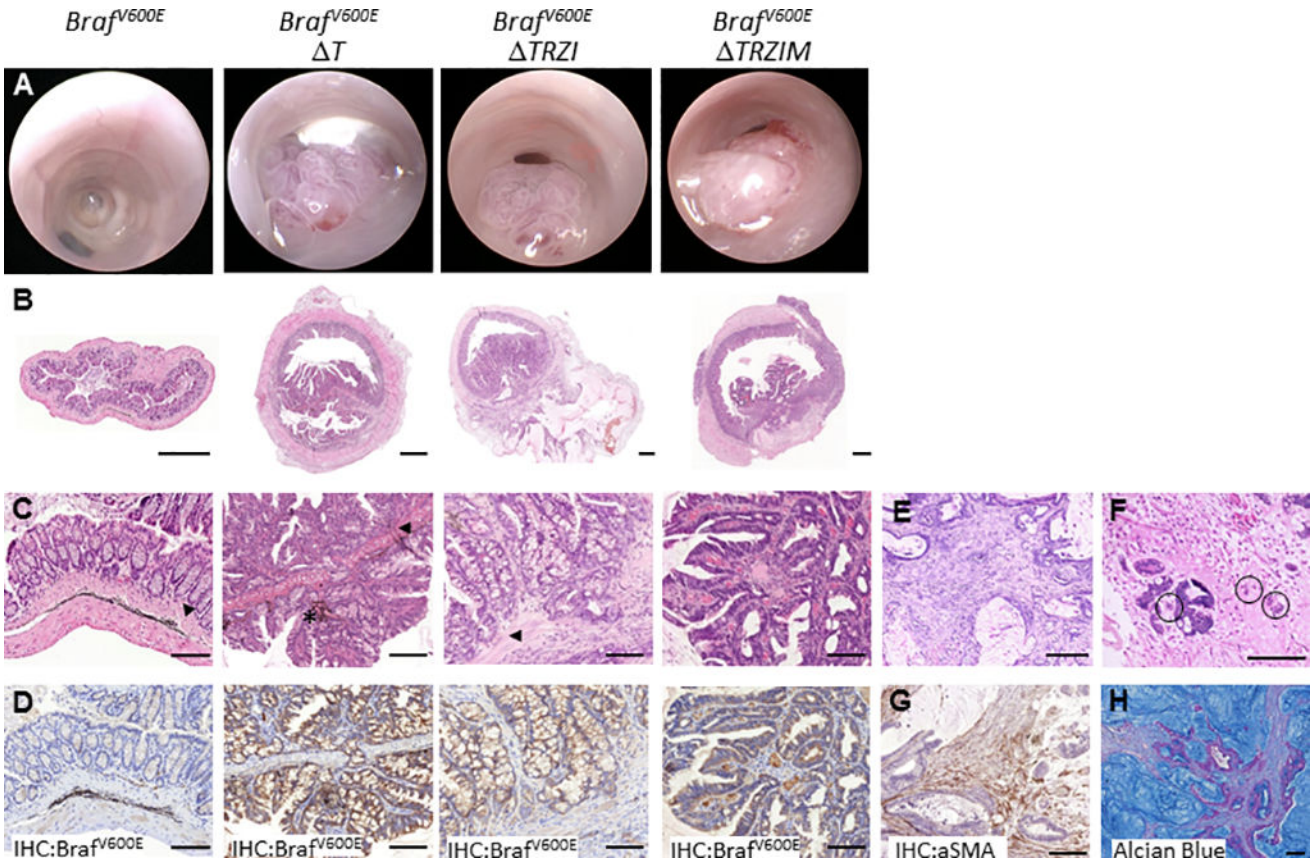

Figure 4. Multi-hit 'serratoids' generate invasive adenocarcinoma with features of human serrated CRC

Colonoscopy **(A)** and histology **(B–H)** images of mouse colon orthotopically injected with mutant organoid lines *Braf*^{V600E}, *Braf*^{V600E} *ΔT*, *Braf*^{V600E} *ΔTRZI*, *Braf*^{V600E} *ΔTRZIM.* **B,** H&E stained sections of whole colon. **C,** higher magnification H&E, arrows denote position of muscularis mucosae, * denotes remnant ink from injection. **D,** immunohistochemical staining for mutant Braf^{V600E} protein clearly delineates serratoid derived tumour cells. **E,** representative images of desmoplastic stromal response and **F,** tumour budding (circled). **G,** tumour stromal response stains positive for alpha-smooth muscle actin (aSMA). **H,** mucin lakes present in mucinous adenocarcinoma visualised using Alcian Blue stain. Scale bars are (B) 500um, (C–H) 100um.

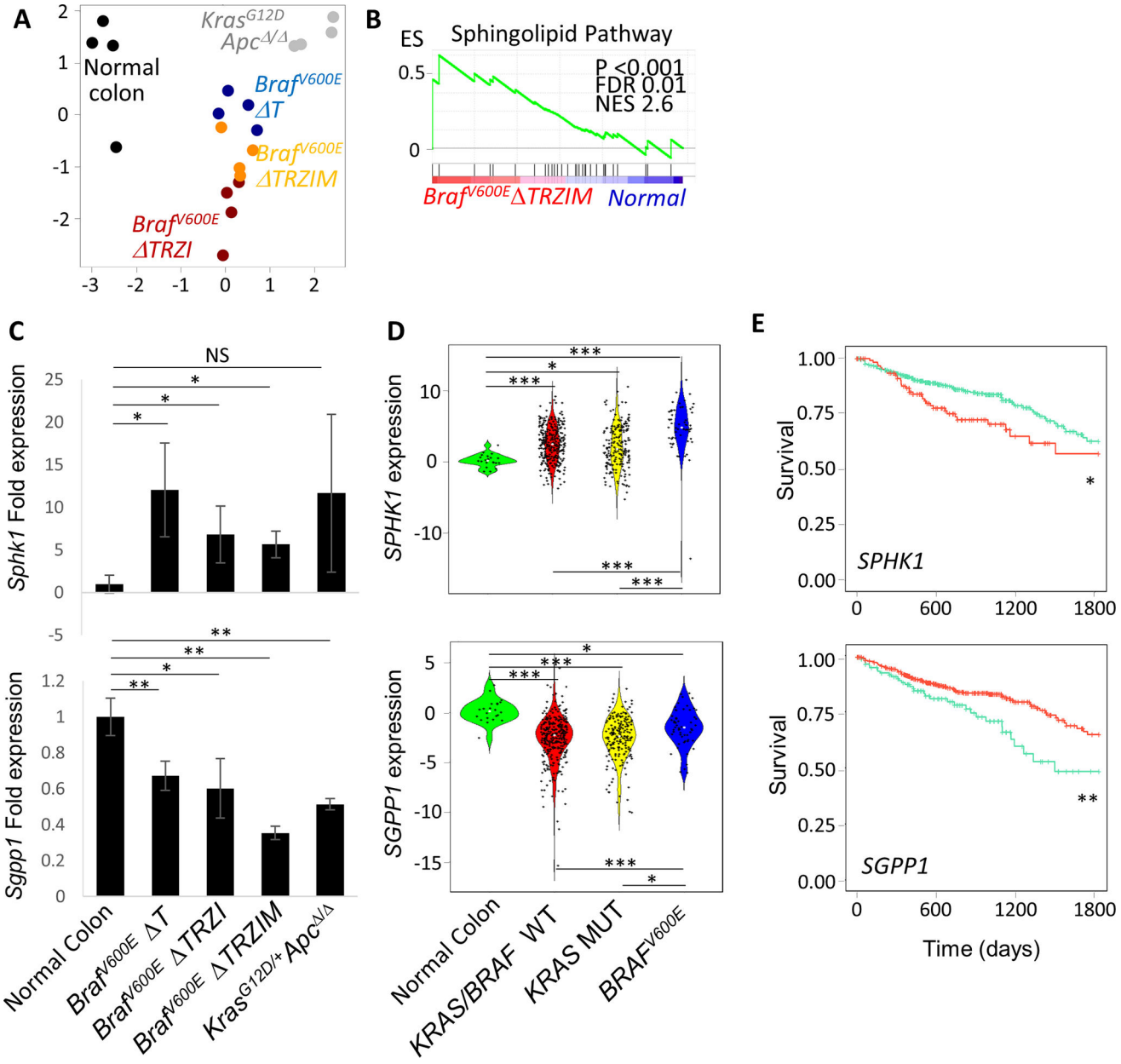

Figure 5. Serrated pathway tumours are molecularly distinct from conventional pathway tumours

A, multi-dimensional scaling plot of RNA expression data from normal mouse colon (black), serrated pathway *Braf*^{V600E} *ΔT* (blue), *Braf*^{V600E} *ΔTRZI* (red) and *Braf*^{V600E} *ΔTRZIM* (yellow) and conventional pathway tumours *Kras*^{G12D};*Apc*$^{Δ/Δ}$ (grey), n=4 samples per group. **B,** gene set enrichment analysis (GSEA) for Sphingolipid *de novo* biosynthesis Reactome between *Braf*^{V600E}*ΔTRZI* serrated tumour and normal mouse colon. Enrichment score (ES), normalised enrichment score (NES), false discovery rate (FDR). **C**, Expression of *Sphk1* is increased and *Sgpp1* is decreased in mouse *Braf*^{V600E} serrated CRC compared to normal mouse colon. Fold induction of mRNA expression is normalized to *Gapdh*, with transcript level in normal colon set to 1. Results from at least four animals with triplicate

technical replicates are shown, error bars denote standard deviation. Two-tailed t-test used for pair-wise statistical analysis. **D,** Violin plots depicting z-score values for normalized expression of *SPHK1* (top) and *SGPP1* (bottom) transcripts in 622 human TCGA CRC and normal colon samples separated into wild-type *BRAF/KRAS*, *KRAS* mutant and $BRAF^{V600E}$ CRC. **E,** Kaplan-Meier plots showing TCGA patient survival probability based on expression level of *SPHK1* (top, *SPHK1* high group n=139 in red, low group n=483 in green) or *SGPP1* (bottom, *SGPP1* low group n=145 in green, high group n=477 in red). *=p≤0.05, **=p≤0.01, ***=p≤0.001, NS= not significant.